2004

A Universal Simulation Tool for Reed Valve Dynamics

Gunther Machu
Hoerbiger Kompressortechnik Services GmbH

Maximilian Albrecht
Vienna University of Technology

Olaf Bielmeier
Hoerbiger Kompressortechnik Schongau GmbH

Thomas Daxner
Vienna University of Technology

Peter Steinruck
Hoerbiger Kompressortechnik Services GmbH

A UNIVERSAL SIMULATION TOOL FOR REED VALVE DYNAMICS

G. MACHU[1], M. ALBRECHT[3], O. BIELMEIER[2], T. DAXNER[3] and P. STEINRÜCK[1]

[1]HOERBIGER Kompressortechnik Services GmbH
Braunhubergasse 23, A-1110 Vienna, Austria
Tel.: +43 1 74004 157, ma@hkts.hoerbiger.com

[2]HOERBIGER Kompressortechnik Schongau GmbH
Im Forchet 5, D-86956 Schongau, Germany
Tel.: +49 8861 210 3386, olaf.bielmeier@hoerbiger.com

[3]Institute of Lightweight Design and Structural Biomechanics
Vienna University of Technology / Austria
A-1040 Vienna, Gusshausstrasse 27-29
Tel.: +43 1 58801 31710, daxner@ilsb.tuwien.ac.at

ABSTRACT

This paper presents a complete model and its implementation as a software tool for simulating the dynamic behavior of reed valves in compressors. A beam Finite Element model with up to 30 degrees of freedom was developed to cover the natural frequencies of the reed valve in conjunction with a contact model for reed stops of arbitrary shape. This algorithm is coupled with equations for compressor kinematics, lift dependent flow resistance and transient, pulsating flow through the cylinder head chambers and pipes.
Thus, a closed model of the physical situation regarding a flexible reed valve, a solution for the contact problem with reed stops of arbitrary shape, coupled with the pulsating flow in the compressor's chambers and associated up- and downstream piping is available.

1. INTRODUCTION

The paper is organized as follows: the next section describes all governing equations and the assumptions of the theoretical modeling. In the successive section a PC based computer software is presented which is based upon this modeling, the LVTKK program. It is designed as an everyday tool for valve designing application engineers. As mentioned above this software is nearly independent from geometrical restrictions so valves with any reed shape and reed stop shape can be simulated. In the last section, the theoretical predictions are compared to measurements which were made on an in-house compressor. As a conclusion, with this model the effects of different reed stops on the dynamic behavior of the valve can be judged along with the interaction of the reed valve with the pulsating flow in the pipeworks and chambers of the compressor.

2. THEORETICAL MODELING

2.1. Compressor Model - Kinematics, Change of State of Cylinder Pressure

As the equations which describe the change of state of the gas inside the cylinder are well known since the late 40's of the last century, it is not necessary to go into much detail here.
Two factors account for the change of state of the gas: (1) the kinematics of the mechanical drive of the compressor, (2) influx/efflux through suction or discharge valve. The position $z(\theta)$ of the piston with respect to crank angle θ is given by (Frenkel, 1969)

$$z(\theta) = \frac{V_c}{A_P} + r(1-\cos\theta) + \frac{r}{\lambda}(1-\sqrt{1-\lambda^2\sin^2\theta}) \qquad (1)$$

From the ideal equation of state the cylinder pressure at any time with respect to θ is

$$p(\theta) = m\frac{RT(\theta)}{A_P z(\theta)} \qquad (2)$$

At the moment of discharge, the temperature, pressure and mass are T_K, p_K and m_K respectively. The gas velocity through an open valve follows from the pressure ratio across the valve (Saint Venant Wanzel equation). Differentiating (2) with respect to time and using the identity $\theta = \omega \cdot t$

$$\frac{dp}{d\theta} = -p\frac{\kappa}{\omega}\left(\frac{\omega\frac{dz}{d\theta} + \frac{A_{effSV}}{A_P}v_{SV} + \frac{A_{effDV}}{A_P}v_{DV}}{z}\right) \qquad (3)$$

is obtained (now taking into account both a suction and a discharge valve). A crank angle of 180° corresponds to the bottom dead center, and the velocities v_{Sv}, v_{DV} are positive for outflow, and negative for inflow through the respective valve. A_{eff} denotes the effective flow area at a certain lift of the respective valve (obtained by wind tunnel measurements), named Φ- number in the following.

2.2. Compressor Model - Forces acting on the reed

In spite of the unavailability of a numerical solution of the three dimensional flow field around the reed a basic model for the pressure distribution over the reed surfaces was used, in which the force F acting on the reed is assumed to be uniform and can thus be derived as follows:

$$F = (p_{cyl} - p_H)A_{port} \qquad (4)$$

In equation (4), A_{port} denotes the smallest area of orifices beneath the reed, p_{cyl} the pressure inside the cylinder, and p_H is the pressure in the cylinder head. The pressure p_H is calculated with the transient flow model.

2.3. Compressor Model - The Transient Flow Model

Especially in the case of low mass reed valves, the calculation of transient flow pulsations proves to be indispensable. Calculations show that the power consumption and especially the delivery rate of compressors are severely influenced by even moderate changes to the piping system. Hence, it is necessary to solve the equations of motion of fluid dynamics. If we assume a one dimensional, instationary, frictionless and adiabatic gas flow in a piping system with variable cross section, the following conservative form of the Euler equations is suitable (see also Anderson, 1995):

Continuity equation: $$\frac{\partial(\rho A)}{\partial t} + \frac{\partial(\rho A v)}{\partial x} = 0 \qquad (5a)$$

Euler equation: $$\frac{\partial(\rho A v)}{\partial t} + \frac{\partial(\rho A v^2 + pA)}{\partial x} = p\frac{\partial A}{\partial x} \qquad (5b)$$

In (5a) and (5b) $\rho(x,t)$ denotes the density of the gas, $v(x,t)$ and $p(x,t)$ the velocity and pressure, and $A(x)$ is the variable cross section in the piping system. From the aforementioned assumptions follows that the change of state of the gas can be modeled as an isentropic change (if there are no shocks in the system). In order to solve (5a) and (5b) simultaneously a variant of the Lax – Wendroff method is programmed, namely the MacCormack scheme, which is of second order in both space and time.

The geometry of the piping system has to be stored in *A(x)* as the area with respect to the x-coordinate. For numerical stability reasons it proves useful to smooth sudden jumps in area by using a smoothing function. Also it is necessary to prescribe an initial temperature, velocity, and pressure at every node point.

Problems arise in the context of the temperature in the piping system. The cylinder head might be water-cooled, that is, there will be heat losses along the pipeworks, resulting in a temperature gradient, etc.. A wrong temperature in the system directly affects the speed of sound, resulting in a delayed or to premature reflection of the pressure pulses from the boundary, thus leading to a different picture. Here, no temperature gradients were accounted for.

The flow conditions in the pipeworks will be subsonic, therefore it is necessary to prescribe one variable (e.g. the pressure) at the boundary, and let the other variable (e.g. velocity) float. There are several different possibilities of conditions at the boundary. In the following, 'left boundary' is always on the cylinder (valve) side, and 'right boundary' describes the end of the piping system (open end, air filter, pressure vessel, etc…).

Table 1: Boundary conditions & Time Step of the Flow Model

	Right Boundary	Left Boundary
Closed valve	velocity extrapol., pres. = ambient + losses	velocity = 0, pressure mirrored
Open valve	velocity extrapol., pres. = ambient + losses	velocity prescribed via Bernoulli,pressure mirrored

An analysis of stability of the governing fluid dynamic equations reveals a stability criterion for the space and timewise discretization, the Courant Friedrichs Levy criterion (CFL):

$$\Delta t = C \frac{\Delta x}{\max\left(|a| + |u|\right)} \qquad (9)$$

where a … local speed of sound, u … local velocity and C … Courant number. For a Courant number $C \leq 1$ stable solutions are obtained.

For the finite element part described in the following, a much smaller timestep is obtained. In order to account for this fact, the program uses the fluid dynamics time step as the global timestep, but the finite element routine has its own local timestep according to the CFL criterion. This procedure saves significant computation time, as valve dynamics only happen in a segment of one crankshaft revolution.

2.4. The Finite Element Model of the Reed Valve

The mechanical part of the problem comprises the thin steel reed, which serves as valve allowing only for one possible direction of flow, as well as the seat and the reed stop, both of which are assumed to be rigid, and both of which constrain the otherwise free movement of the reed. The dynamic deformation of the reed was predicted by means of the Finite Element method (Bathe, 1995 & Hughes, 2000), the infinite number of degrees-of-freedom for the continuum problem being reduced to a finite number of translational (u_i) and rotational degrees-of-freedom φ_i by discretizing the reed with non-standard Hermite beam-elements.

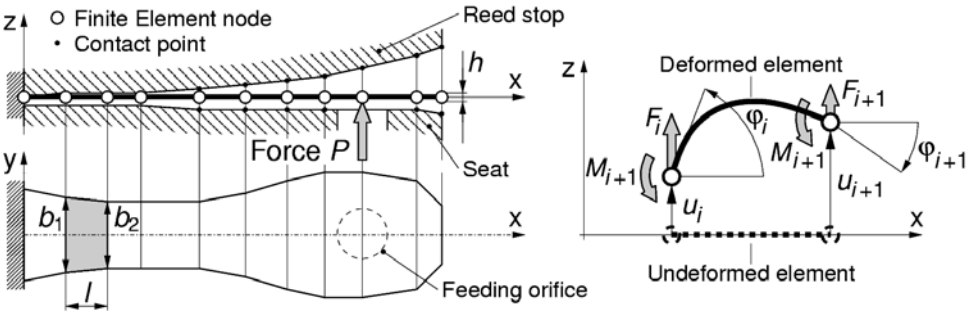

Figure 1: Schematic layout of the Finite Element model.

Figure 1 shows the general layout of the Finite Element model. At one end ($x = 0$) the reed, which represents a cantilever beam with constant thickness h, but varying width, is fully constrained. The free part of the reed is discretized by a number of beam Finite Elements with a piecewise linear width distribution $b(x)$ changing from b_1 to b_2 over the element length l. Third-order, Hermite polynoms are used as the elements' shape functions. The coefficients of the stiffness matrix $\mathbf{K}_{el}$, which couples the vector of element degrees-of-freedom $\mathbf{u}_{el} = [u_i, \varphi_i, u_{i+1}, \varphi_{i+1}]^T$ and the vector of element forces and moments $\mathbf{F}_{el} = [F_i, M_i, F_{i+1}, M_{i+1}]^T$ as defined in Figure 1, are chosen to provide a best-fit of the actual higher-order deflection function for a beam element with linear width distribution $b(x)$. From the static element equilibrium equation $\mathbf{F}_{el} = \mathbf{K}_{el}\mathbf{u}_{el}$ the stiffness matrix follows as

$$\mathbf{K}_{el} = \frac{E}{l^3}\frac{h^3}{12}\begin{bmatrix} 6(b_1+b_2) & 2(2b_1+b_2)l & -6(b_1+b_2) & 2(b_1+2b_2)\,l \\ & (3b_1+b_2)l^2 & -2(2b_1+b_2)\,l & (b_1+b_2)\,l^2 \\ & & 6(b_1+b_2) & -2(b_1+2b_2)\,l \\ \text{sym.} & & & (b_1+3b_2)\,l^2 \end{bmatrix} \tag{6}$$

In Equation (6) E denotes the Young's modulus of the reed valve material, and the node indices i and $i + 1$ were substituted with 1 and 2, respectively, for better readability.
After summing up the element stiffness matrices $\mathbf{K}_{el}$ to obtain the global system stiffness matrix $\mathbf{K}$, the system's equations of motion can be expressed in matrix notation as

$$\mathbf{M}\frac{d^2\mathbf{u}}{dt^2} + \mathbf{C}\frac{d\mathbf{u}}{dt} + \mathbf{K}\mathbf{u} = \mathbf{F} \tag{7}$$

where $\mathbf{u}$ denotes the vector of nodal displacements, **M** is the lumped mass matrix of the system, **C** is a diagonal damping matrix representing external damping forces, and **F** symbolizes the vector of external nodal forces and moments. The latter vector of generalized forces contains contributions from internal(material) damping effects, contact forces as well as the force resultant P of the gas pressure distribution above the feeding orifice.

The system of differential equations (7) is integrated by means of an explicit, central difference integration scheme, which is computationally efficient as long as the matrices **M** and **C** are diagonal. Since this procedure is only conditionally stable appropriate measures have to be taken to keep the time step below a mesh-dependent critical size. The stability criterion

$$\Delta t_{crit} < \frac{T_{min}}{\pi}, \tag{8}$$

where Δt_{crit} is the maximum admissible time step size and T_{min} is the shortest period of oscillation in the system, was fulfilled by approximating T_{min} to the shortest oscillation period among all individual elements.
The kinematic constraints imposed by the contact conditions between the lamellae and the surrounding rigid structures were enforced by the penalty method, for which stiff, compression-only springs prevent an excessive interpenetration of the parts in contact.
Pre-tensioned reeds were taken into account by allowing for a non-straight neutral beam axis in the unconstrained configuration. The amount of pre-tensioning was determined by the radius of curvature in this configuration. Stacked lamellae were also accounted for.

The proposed Finite Element system was implemented as a program module of the LVTKK program. The pressure force F is the principal input quantity while the valve lift is the most important output parameter. Through the latter two variables the coupling between the fluid dynamics part and the structural dynamics part is obtained.

3. IMPLEMENTATION AS A COMPUTER PROGRAM

Transferring the developed model into computer code is a straight forward procedure. But to use this program for daily's work valve designing requires much more. There shouldn't be any basic limitations on the geometrical shape of reed and reed stop or number of reeds to be handled. These reed data together with other valve and compressor related information (e.g. Φ-number-functions according to Soedel (1992), material, speed, stroke) are stored in a central database. Every registered user can create his own set of calculations (named calculation sheet) having a unique reference number. A sophisticated data handling and managing system guarantees that no double reference numbers occur even when there's no access to the central data base (e.g. remote laptop system). The fully implemented simulation (see screenshot above) module and a detailed documentation system of the obtained results (printout, file) makes it a valuable tool for both application engineer and customer.

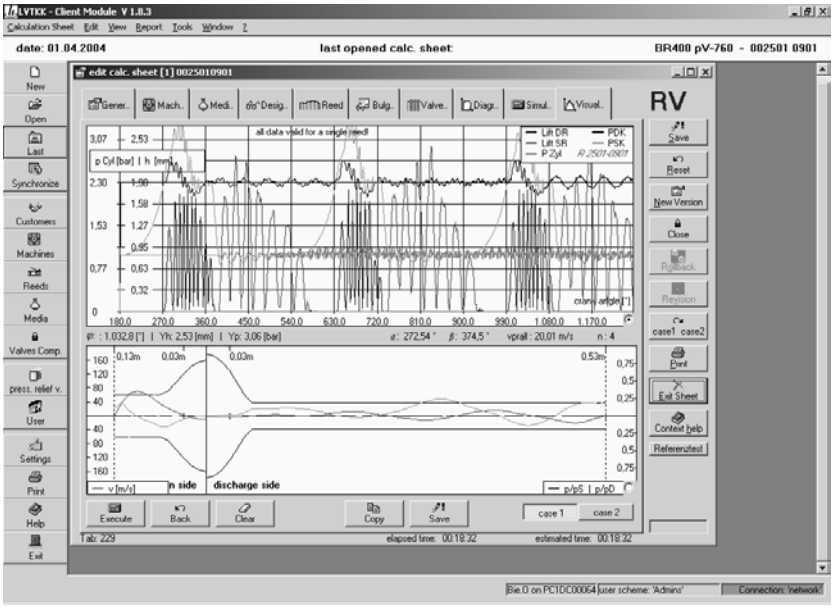

Figure 2: Screenshot of software output (valve simulation).

4. COMPARISON OF SIMULATIONS VS. MEASUREMENTS

In order to evaluate the computer code, measurements have been made to check the results of the simulation with real compressor valve behavior.
An brake-air compressor (courtesy of DaimerChrysler) with water-cooled valve was used for gauging at variable speed and pressure levels:

Table 2: valve and compressor data.

bore / stroke:	100 / 46 mm	valve data:	lift SV (at tip):	0.6 mm	lift DV:	1.9 mm
pressure:	1 – 13 bar		gap area SV:	1.36 cm^2	gap area DV:	2.39 cm^2
speed:	500 rpm – 2500 rpm		Φ-number SV:	0.94 cm^2	Φ-number DV:	1.80 cm^2

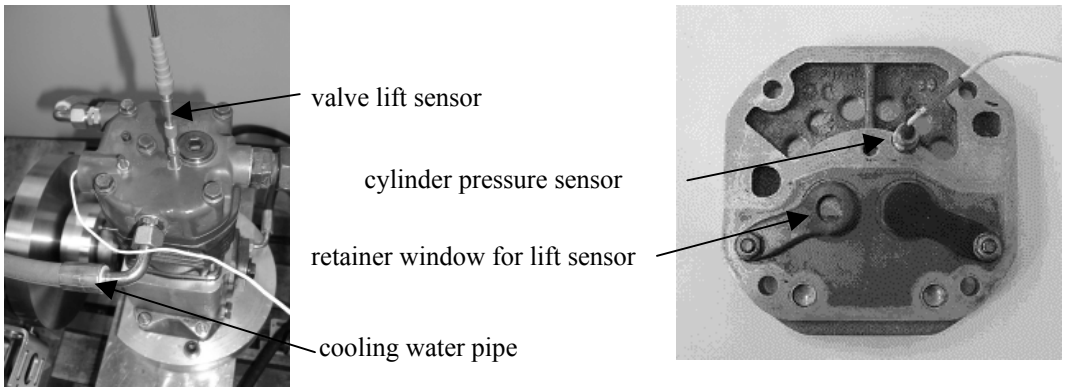

Figure 3: Experimental set-up.

Besides some equipment to gather compressor condition (speed, crank angle, working pressure etc.) an optical valve movement analyzer (OVM), developed and designed by HOERBIGER, was used to quantify reed lift (see figure 3). Data acquisition was performed with a common PC-based system. The system is triggered by the TDC signal that only one cycle is displayed continuously on the monitor. This yields all the information needed and helps to see if valve movement is stable.

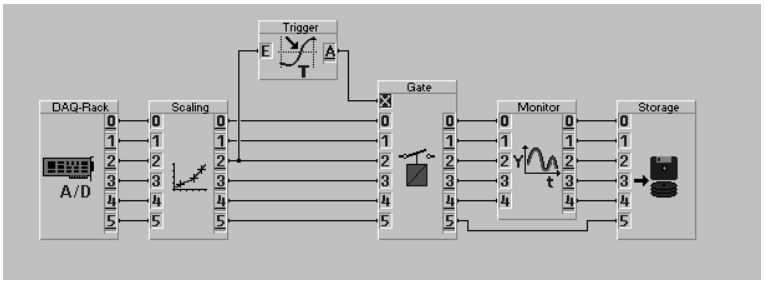

sampling frequency: 5 kHz per channel
cyl. pressure sensor sensitivity: 5 mV/bar
resolution OVM: 40 µm
reproducibility OVM: ± 0.1 mm

Figure 4: Data acquisition layout.

For the calculations suction and discharge chamber volumes were taken into account with their corresponding cross sections as well as the geometry of the connection pipes.
As the backlash of pressure waves on the valves is very sensitive to the pulsation geometry, calculation accuracy depends on correct geometry data.
Two examples with extremely different working conditions (i.e. discharge pressures, atmospheric suction pressure) are used to demonstrate the predictability of valve parameters determined by this software:

Table 3: working conditions of compressor.

case 1:	speed 500 rpm	working pressure 1.1 bar
case 2:	speed 2500 rpm	working pressure 12.7 bar

4.1. Lift diagrams

Common to all following diagrams is that simulation starts at bottom dead center (BDC). Therefore the discharge valve is displayed first.
The valve used for the measurements has end to end reed stops on discharge side but only a lift-pocket for the suction reed. For this reason the maximum elevation above seat level can exceed the determined lift (see sequence below):

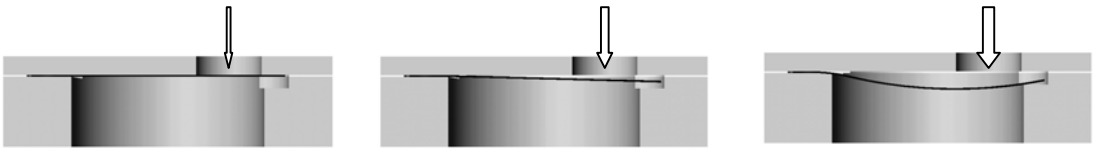

closed ... beginning opening ... ... tip at stop, reed flexing further

Figure 5: suction reed movement.

In the low speed case the observed and calculated fluttering frequency match very closely (see figure 6). However the height of measured lift pattern doesn't exactly reach the measured one. As the FE model contains a lot of experimentally undetermined parameters (especially those for damping properties) a widespread set of measurements could help to improve compliance.
For the high speed case the damping behavior at reed stop is of less importance because of the large flow forces acting on the reed. Therefore the real and simulated lift height of discharge valve correspond. The fact that there is more substructure observable in the software generated pattern than in the measured one could be up to the limited time resolution of the data acquisition system; any details present are blurred in the resulting graph.

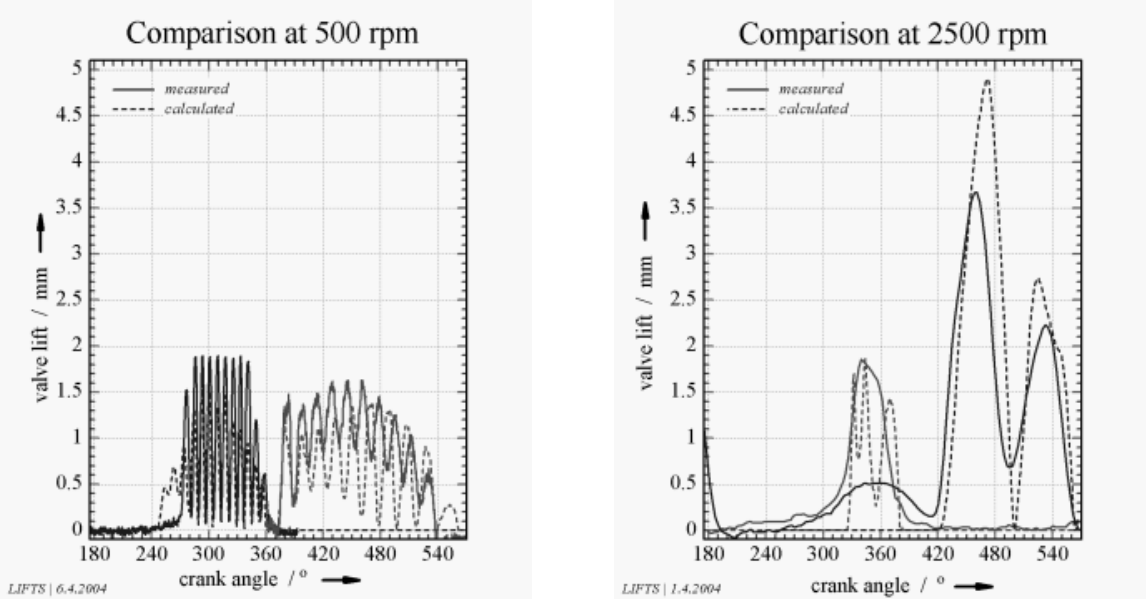

Figure 6: suction reed movement, lift diagrams.

On the inlet side a large lift is observed according to the effect illustrated in figure 5. That the calculated lift is even bigger could be attributed to the nonlinear nature of the OVM scaling (it is designed for small lift only). But despite these shortcomings the general valve behavior is well predicted.

4.2. Cylinder pressure diagrams

On looking at the cylinder pressure diagrams the difficulties in predicting pulsation effects correctly become obvious: although the march of pressure is reproduced very well by the numerical calculation pressure drops too fast in both cases after opening of the discharge valve. That observation is related to the fact that no pressure losses at sudden changes of the cross section are modeled.
But for an evaluation of valve behavior the obtained results are very satisfying.

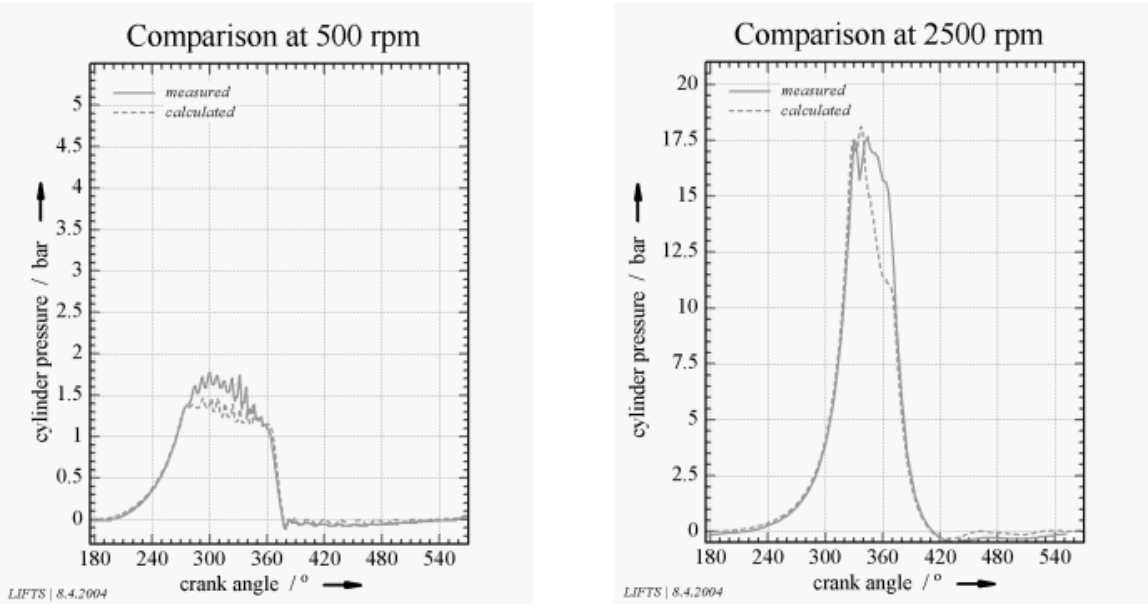

Figure 7: cylinder pressure diagrams.

5. CONCLUSIONS

- The desired goal to develop a universal design and simulation tool for reed valves has been achieved. Although the program contains a lot of pre-defined parameters (e.g. reed shapes, drill hole geometries, Φ-number functions) the application engineer still has enough freedom to create a custom valve design.
- Simulated and measured pressure and lift traces match very closely. It may be concluded that the physical situation is described with great detail.
- The database concept and the modular structure of the LVTKK program yields the necessary flexibility to meet future requirements.

NOMENCLATURE

V_c	clearance volume	(cm^3)
A_P	piston area	(cm^2)
r	crankshaft radius	(mm)
λ	crankshaft ratio	()
ω	frequency	(s^{-1})
κ	specific heat ratio	()
A_{eff}, Φ-number	effective flow area	(cm^2)
A_{port}	port area	(cm^2)
v	gap velocity	(m/s)
ρ	density of gas	(kg/m^3)
u	displacement	(mm)
a	local speed of sound	(m/s)
TDC	top dead center	

Subscripts

SV	suction valve
DV	discharge valve
cyl	cylinder
H	cylinder head

REFERENCES

Anderson, J.D, 1995, *Computational Fluid Dynamics*, McGraw-Hill Inc., New York , p. 77-78.

Bathe, Klaus-Jürgen, 1996, *Finite Element Procedures*, Prentice-Hall, Upper Saddle River, NJ.

Frenkel, 1969, *Kolbenverdichter*, VEB Verlag Technik, Berlin, 177 p.

Hughes, T.J.R., 2000, *The Finite Element Method*, Dover Publications, Mineola, NY.

Soedel, Werner, 1992, *Mechanics, Simulation and Design of Compressor Valves, Gas Passages and Pulsation Mufflers,* PURDUE University, West Lafayette, p. 30-36